Received: 13 May 2023 | Revised: 17 August 2023 | Accepted: 8 October 2023

DOI: 10.1111/gcb.17007

Global Change Biology WILEY

RESEARCH ARTICLE

# Blue carbon sink capacity of mangroves determined by leaves and their associated microbiome

Zhe Lu[1,2] | Guoming Qin[1,3] | Shuchai Gan[1,2] | Hongbin Liu[4] | Peter I. Macreadie[5] | Wee Cheah[6] | Faming Wang[1,2]

[1]Xiaoliang Research Station of Tropical Coastal Ecosystems, Key Laboratory of Vegetation Restoration and Management of Degraded Ecosystems, the CAS Engineering Laboratory for Ecological Restoration of Island and Coastal Ecosystems, and Guangdong Provincial Key Laboratory of Applied Botany, South China Botanical Garden, Chinese Academy of Sciences, Guangzhou, P.R. China

[2]South China National Botanical Garden, Guangzhou, P.R. China

[3]University of Chinese Academy of Sciences, Beijing, P.R. China

[4]Department of Ocean Sciences and Division of Life Sciences, School of Science, Hong Kong University of Science and Technology, Hong Kong, P.R. China

[5]School of Life and Environmental Sciences, Deakin University, Burwood Campus, Burwood, Victoria, Australia

[6]Institute of Ocean and Earth Sciences, Universiti Malaya, Kuala Lumpur, Malaysia

**Correspondence**
Faming Wang, Xiaoliang Research Station of Tropical Coastal Ecosystems, Key Laboratory of Vegetation Restoration and Management of Degraded Ecosystems, the CAS Engineering Laboratory for Ecological Restoration of Island and Coastal Ecosystems, and Guangdong Provincial Key Laboratory of Applied Botany, South China Botanical Garden, Chinese Academy of Sciences, Guangzhou 510650, P.R. China.
Email: wangfm@scbg.ac.cn

**Funding information**
2022 CAS Project for Young Scientists in Basic Research, Grant/Award Number: YSBR-037; ANSO collaborative research, Grant/Award Number: ANSO-CR-KP-2022-11; Australian Research Council Discovery Grant, Grant/Award Number: DP200100575; Basic and Applied Basic Research Foundation of Guangdong Province, Grant/Award Number: 2021B1212110004, 2021B1515020011 and 2023A1515010946; Natural Resources Affairs Management-Ecological Forestry Construction Special Project of Forestry Administration of Guangdong Province, Grant/Award Number: 2022-8; CAS Youth Innovation Promotion Association, Grant/Award Number: 2021347; Key Laboratory of Vegetation Restoration and Management of Degraded Ecosystems, South China Botanical Garden, Chinese Academy of Sciences, Grant/Award Number: VRMDE2204; Key-Area Research and Development Program of Guangdong

## Abstract

Mangroves play a globally significant role in carbon capture and storage, known as blue carbon ecosystems. Yet, there are fundamental biogeochemical processes of mangrove blue carbon formation that are inadequately understood, such as the mechanisms by which mangrove afforestation regulates the microbial-driven transfer of carbon from leaf to below-ground blue carbon pool. In this study, we addressed this knowledge gap by investigating: (1) the mangrove leaf characteristics using state-of-the-art FT-ICR-MS; (2) the microbial biomass and their transformation patterns of assimilated plant-carbon; and (3) the degradation potentials of plant-derived carbon in soils of an introduced (*Sonneratia apetala*) and a native mangrove (*Kandelia obovata*). We found that biogeochemical cycling took entirely different pathways for *S. apetala* and *K. obovata*. Blue carbon accumulation and the proportion of plant-carbon for native mangroves were high, with microbes (dominated by *K*-strategists) allocating the assimilated-carbon to starch and sucrose metabolism. Conversely, microbes with *S. apetala* adopted an *r*-strategy and increased protein- and nucleotide-biosynthetic potentials. These divergent biogeochemical pathways were related to leaf characteristics, with *S. apetala* leaves characterized by lower molecular-weight, C:N ratio, and lignin content than *K. obovata*. Moreover, anaerobic-degradation potentials for lignin were high in old-aged soils, but the overall degradation potentials of plant carbon were age-independent, explaining that *S. apetala* age had no significant influences on the contribution of plant-carbon to blue carbon. We propose that for introduced mangroves, newly fallen leaves release nutrient-rich organic matter that favors growth of *r*-strategists, which rapidly consume carbon to fuel growth, increasing the proportion of microbial-carbon to blue carbon. In contrast, lignin-rich native mangrove leaves shape *K*-strategist-dominated microbial communities, which grow slowly and store

  

Province, Grant/Award Number: 2022B1111230001; National Forestry and Grassland Administration Youth Talent Support Program, Grant/Award Number: 2020BJ003; National Key Research and Development Program of China, Grant/Award Number: 2021YFC3100402; National Natural Science Foundation of China, Grant/Award Number: 32301398, 32011530164, 32171594, 42007230 and U2106209; R & D program of Guangdong Provincial Department of Science and Technology, Grant/Award Number: 2018B030324003; South China Botanical Garden, Chinese Academy of Sciences, Grant/Award Number: QNXM-08

assimilated-carbon in cells, ultimately promoting the contribution of plant-carbon to the remarkable accumulation of blue carbon. Our study provides new insights into the molecular mechanisms of microbial community responses during reforestation in mangrove ecosystems.

**KEYWORDS**
biogeochemistry, blue carbon, carbon cycling, coastal ecosystem, FT-ICR-MS, functional potential, mangrove restoration, metagenome sequencing, microbial biomass, microbiome

## 1 | INTRODUCTION

Mangroves are among the most carbon (C)-rich ecosystems on earth, providing immense ecological services for C storage (Adame et al., 2021; Macreadie et al., 2021; Wang et al., 2020). Along with salt marshes and seagrasses, these coastal wetlands were considered blue C ecosystems (BCEs), and play a crucial role in mitigating climate change (Bertram et al., 2021; Wang et al., 2023). Globally, there is a growing interest in BCEs as a natural climate solution for offsetting greenhouse gas emissions through preservation and restoration efforts (Donato et al., 2011; Macreadie et al., 2019; Sanders-DeMott et al., 2022; Wang et al., 2021). Unfortunately, mangroves have been adversely impacted by anthropogenic activities since the 1950s.

In China, for example, the mangrove area has decreased from 50,000 ha in the 1950s to 15,000 ha in 1990 (Ren et al., 2009). Afforestation has been identified as an effective way for mitigating these losses and enhancing ecosystem services (Macreadie et al., 2021). It is important to note that mangrove soil harbors 49%–98% of carbon in these ecosystems (Donato et al., 2011; Liang, 2020; Mambelli et al., 2011). Moreover, the relative contribution of externally-produced C ('allochthonous') versus self-produced C ('autochthonous') to mangrove blue C stocks varies widely (Canuel & Hardison, 2016; Hiraishi et al., 2014; Kramer et al., 2017). Thus, understanding soil C cycling is critical for restoring belowground ecosystem structure and function during afforestation efforts (Bardgett & van der Putten, 2014). However, little is known about how afforestation regulates the microbial-driven transfer of C from plant litter to the underlying soil horizons in mangroves.

Microbes with different growth strategies determine how plant-derived C is decomposed and incorporated into soil organic C (SOC) (Cotrufo et al., 2013; Liang et al., 2017). Microbial communities can differentiate into communities dominated by *r*- and *K*-strategists, respectively, depending on the forms and concentration of ambient C (Chen et al., 2016; Schneckenberger et al., 2008). *R*-strategists dominate when labile C is abundant, allocating plant-derived C to energy and biosynthesis processes (protein/nucleotides biosynthesis) for rapid growth (Blagodatskaya & Kuzyakov, 2008; Malik et al., 2020). In contrast, *K*-strategists dominate when labile C is scarce, and they secrete enzymes to decompose recalcitrant C and store the plant-derived C primarily in the form of polysaccharides, contributing to SOC accumulation and stabilization (Prosser et al., 2007). In mangrove, the organic matter in soil mainly originate from litterfall (Alongi, 2014; Kristensen et al., 2008). Hence, the tree species used for afforestation have far-reaching influence on the microbial-driven SOC formation and stabilization due to the distinct characteristics of their leaf litter C.

In terrestrial ecosystems, plant litter C is aerobically decomposed and assimilated into microbial biomass (Dignac et al., 2005; Dungait et al., 2012; Robertson et al., 2008), contributing to SOC formation (Marschner et al., 2008; Sayer, 2006; Xu et al., 2013). However, unlike terrestrial ecosystems, mangroves are periodically exposed to tidal inundation, and undergo highly complex redox reactions (Arndt et al., 2013). These fluctuating redox conditions closely determine the decomposition of plant litter C (mainly lignin, cellulose, hemicellulose, etc.) in mangroves, which may differ from terrestrial ecosystems (Dittmar & Lara, 2001; Leadbeater et al., 2021; Marchand et al., 2005). As previously demonstrated, anaerobic degradation of plant litter C is significant in waterlogged sediments (Yu et al., 2018). Hence, an integrated assessment of anaerobic and aerobic degradation potential of the plant litter C is crucial to understand its contribution to SOC formation.

To efficiently restore the degraded mangroves, *Sonneratia apetala*, a pioneer species with high adaptability and growth rate, was introduced in China (Ren et al., 2008). Previous studies have shed some light on the impacts of introducing *S. apetala* on the biodiversity, and SOC storage in mangrove ecosystems (Ren et al., 2010; Soares & Schaeffer-Novelli, 2005). However, two major issues remain unresolved. First, the leaf litter of the introduced *S. apetala* and the long-growing native species *Kandelia obovata*, differ significantly, such as in cellulose-to-lignin ratio (Rao et al., 2021), but little is known about their differences in characteristics of leaf dissolved organic matter (DOM) and their effects on microbial-driven SOC sequestration. Second, during afforestation, litterfall forms layers on the topsoil, creating potential anaerobic micro-environments (Huang & Spohn, 2015; Leitner et al., 2016), but it is unclear whether the anaerobic lignin degradation in soils becomes more significant with the increasing age of *S. apetala*, thereby changing the contribution of plant litter C to SOC storage.

Here, we integrated Fourier-transform ion cyclotron resonance mass spectrometry (FT-ICR-MS), soil carbon component analysis, and metagenome sequencing to clarify the variability in leaf characteristics, soil lignin contents, and soil microbial communities of *S. apetala* compared with the native species/tidal flat on Qi'ao Island in South China. FT-ICR-MS, a cutting-edge technology, allowed precise characterization of diverse DOM formulas (Blackburn et al., 2017; Gan et al., 2021). We hypothesize that (1) *S. apetala* leaf DOM has a lower molecular weight than native species, and shapes the soil microbial communities dominated by *r*-strategists, leading to greater partitioning of plant-derived C to microbial growth and division, rather than storage; (2) old-aged *S. apetala* soils exhibit higher lignin anaerobic degradation potentials due to the thicker litter layer. The island of Qi'ao was selected as a suitable location for investigating the potential of *S. apetala* and *K. obovata* soils as blue C sinks. This choice was based on the similarity of the tidal flats where both species were planted and the sediments environments they encountered (Yu et al., 2020). We believe that our findings provide insights into the molecular mechanisms of microbial community responses during mangrove reforestation.

## 2 | MATERIALS AND METHODS

### 2.1 | Study site and soil sampling

We conducted leaf, pedological, and microbial investigations in June 2022 at a sampling site located in Qi'ao Mangrove Wetland Park (22°26′ N, 113°38′ E), Guangdong Province, China. The average temperature is 22.4°C, and the average annual precipitation is 1700–2200 mm, with most occurring between April and September (Yu et al., 2020). The tides are irregularly semidiurnal, with mean high and low tides of 0.17 and −0.14 m, respectively (Chen et al., 2014). The soils are mainly coastal sandy soil. Due to large-scale deforestation from 1984 to 1998, only a small proportion of the native mangrove species *Kandelia obovata* remains, with *S. apetala* becoming dominant since 1999 (Yu et al., 2020).

Soil samples were collected from four different sites: tidal flat control (CK), 10-year-old *S. apetala* (SA10), 20-year-old *S. apetala* (SA20), and 40-year-old *K. obovata* (KO). They were planted on tidal flats with similar tidal levels (1.45–1.55 m) and flooding duration time (10.3–10.6 h). Each site had four sampling plots (10 × 10 m) with similar initial conditions in terms of tide level and elevation, which were ensured using a surface elevation table. Each plot was randomly distributed within each site and separated from others by more than 10 m. For each plot, three soil cores were randomly collected, with 0–10 cm topsoil collected using a steel semi-opened corer (5 cm diameter, 100 cm depth) after removing plant litter. Three core segments from each plot were homogenized to establish a composite soil sample. In total, 12 composite soil samples (3 replicates × 4 sites) were obtained. Each sample was separated into two portions: one was immediately frozen in dry ice in situ and stored at −80°C for analyses of phospholipid fatty acid (PLFA) and metagenomics; and the other portion was air-dried at room temperature for analyses of SOC and lignin content.

### 2.2 | Comparison of leaf DOM and soil microbial communities between *S. apetala* and *K. obovata*

#### 2.2.1 | Leaf sampling and FT-ICR-MS-based characterization

To investigate how the introduced *S. apetala* and native species *K. obovata* regulate SOC formation by altering the composition of soil microbial community, the leaves of *K. obovata* and *S. apetala* and soils from the tidal flat, 10-year-old *S. apetala*, and *K. obovata* were sampled along the intertidal region at the study site. Ten fresh leaves of *S. apetala* and *K. obovata* were randomly picked and freeze-dried. Ten fresh leaves from each species were freeze-dried, ground, and immersed in Milli-Q water (leaf to water mass ratio = 1:10) for 24 h (Hur et al., 2009). The leaf leachate was then filtered and concentrated using tyrene-divinyl-benzene polymer (PPL) cartridges for FT-ICR-MS measurements (Dittmar et al., 2008). FT-ICR-MS analysis was performed on a 7T FT-ICR-MS equipped with an ESI source in negative mode. Detailed leaf treatment, leachate preparation, and FT-ICR-MS detection procedures can be found in the supplementary files.

#### 2.2.2 | Phospholipid fatty acids-based microbial biomass analyses

Soil samples were sieved to 2 mm and used for PLFAs extraction and analysis. PLFAs are important components of microbial cell membranes, rapidly decomposing after cell death, making them indicators to distinguish living from dead organisms (Frostegård & Bååth, 1996). The PLFAs were extracted from 8 g of frozen and sieved soil in a mixture of chloroform, methanol, and phosphate buffer (1:2:0.8, *v*:*v*:*v*), and then evaluated by gas chromatography (GC7890, Agilent, California, USA) after further separation, purification, and methyl esterification of the organic phase (Frostegård et al., 2011). Standard internal peak (C19:0) was used for peak identification, and PLFAs were assigned following standard nomenclature (Tunlid et al., 1989). Biomarker PLFAs were estimated for fungi (18:2ω6c, 18:3ω3c, and 16:1ω5c) and bacteria (i14:0, i15:0, a15:0, i16:0, i17:0 a17:0, 16:1ω7c, 18:1ω9c, 18:1ω7c, 15:0 and 17:0) (Bossio et al., 2006). The total PLFA biomass was calculated as the sum of the fungi, bacteria and PLFAs 14:0, 16:0, 16:1ω5c, and 17:1ω8c (Bardgett et al., 1999).

#### 2.2.3 | Microbial assimilated C partitioning analyses

To analyze the partitioning patterns of assimilated plant-derived C in microbes, we used metagenomics data and calculated total

gene abundances in four pathways (starch and sucrose metabolism, fatty acid biosynthesis, amino acid metabolism, and nucleotide metabolism), all starting with acetyl-CoA as a precursor. Next, we determined the relative changes in pathway abundances in *S. apetala* and *K. obovata* soils by comparing them to the corresponding pathway abundances in tidal flat soils. For example, the gene abundance of the starch and sucrose metabolism pathway in *S. apetala* was divided by the corresponding gene abundance in tidal flat soils.

#### 2.2.4 | Microbial-derived C extraction and quantification

We employed the Indorf et al. (2011) protocol to extract and assess soil amino sugars (glucosamine (GluN), muramic acid (MurN), and galactosamine (GalN)), which are indicators of microbial-derived C. Briefly, 0.5 g of air-dried soil (<2 mm) was subjected to hydrolysis at 105°C for 8 h with 10 mL 6 M HCl, followed by cooling to 25°C and filtration. To eliminate the HCl, 0.5 mL supernatant was evaporated using an evaporator, and the resulting residue was dissolved in ultrapure water and stored at −20°C for quantification and determination of GluN, MurN, and GalN (Liang et al., 2019) (see Supplemental file for details).

### 2.3 | Exploration of the effects of *S. apetala* ages on the lignin degradation and its contribution to SOC

#### 2.3.1 | Soil selection

Given the age discrepancy between the studied *S. apetala* and *K. obovata*, we further investigated whether the age of *S. apetala* influences the degradation potential of plant-derived C and its contribution to SOC. This experiment aimed to eliminate any confounding effects of *S. apetala* age on SOC formation, so as to better compare the distinctions in the SOC formation mechanisms of *S. apetala* and *K. obovata*. We selected a chronosequence of afforestation sites representing over 20 years of restoration: a tidal flat control, 10-year-old *S. apetala*, 20-year-old *S. apetala*. The chronosequence sampling was based on the principle of space-for-time substitution, providing a unique opportunity to study the long-term dynamics of lignin degradation potentials and its contribution to SOC.

#### 2.3.2 | Metagenomics-based analysis of plant C degradation potentials

Details on the DNA extraction, library construction, metagenomic sequencing, genome assembly, and gene prediction can be found in the Supplementary files. Taxonomic annotation of the representative sequences of non-redundant gene was performed using DIAMOND (http://www.diamondsearch.org/index.php, version 0.8.35; Buchfink et al., 2015) combined with NCBI's non-redundant protein (NR) database, with an *e*-value cutoff of 1e-5. Functional annotation was achieved using carbohydrate-active enzymes (CAZymes; Cantarel et al., 2009) and Kyoto Encyclopedia of Genes and Genomes (KEGG, http://www.genome.jp/keeg) databases, also with an *e*-value cutoff of 1e-5. The genes for CAZymes, aerobic- and anaerobic lignin degradation were selected from CAZymes and KEGG databases. Gene abundances were normalized into reads per kilobase of transcript per million mapped reads (RPKM), which is commonly used in metagenomics to counteract the effects of total read counts and gene lengths when comparing the gene abundances between samples.

#### 2.3.3 | Lignin extraction and plant-derived C quantification

Soil lignin phenols were extracted using the alkaline CuO oxidation method following Hedges and Ertel (1982). Briefly, about 1.0 g of air-dried soil samples was mixed with 500 mg CuO, 100 mg $Fe(NH_4)_2(SO_4)_2$ in 15 mL NaOH solution (2 M) in Teflond vessels. After flushing the headspace with $N_2$ for 5 min, the vessels were heated at 170°C for 2 h and kept at room temperature overnight. The CuO-oxidated products were then derivatized at 60°C for 3 h with N,O-bis-(trimethylsilyl) trifluoroacetamide (BSTFA) and pyridine to produce trimethylsilyl (TMS) derivatives (Ma et al., 2018). The derivatives were detected using an Agilent 7890B gas chromatography equipped with a 710B TQ mass spectrometer (Agilent, USA). The lignin phenols were quantified by the total amounts of vanillyl (*V*)-, syringyl (*S*)-, and cinamyl (*C*)-based phenols. The plant-derived C was calculated using Equation (1):

$$\text{Plant} - \text{derived C}\,(\%\,\text{SOC}) = \frac{\left(\frac{V}{33.3\%} + \frac{S}{90\%} + C\right)}{40\% \times \text{SOC}} \times 100\%, \quad (1)$$

where 33.3% and 90% represent the release efficiencies of *V*- and *S*-based phenols, respectively, based on the CuO oxidation method. The value 40% indicates the minimum lignin content found in empirical mangrove residues (Yang et al., 2018).

### 2.4 | Statistical analysis

Data analyses and visualization were performed in *R* (v4.2.0, R Development Core Team, 2009), unless otherwise specified. Gene and species abundances represented by log-transformed RPKMs were used for analyses. Means and standard deviations were shown in figures and tables. Brays–Curtis distance-based principal components analysis (PCA) and analysis of similarity (ANOSIM) were performed using *vegan* and *ggpubr* packages to assess differences in microbial community composition among groups. The differences in log-transformed RPKMs of genes or species among groups were tested using Kruskal–Wallis one-way analysis of variance (Kruskal–Wallis test; function: Kruskal.test). Pairwise differences between genes or species were tested using pairwise Wilcoxon rank-sum test with false discovery rate correction (FDR; function: pairwise.wilcox.

test (x, g, *p*.adjust.method = "fdr"), where x and g represent response and group, respectively).

Visualization of gene and species abundance was achieved using *pheatmap* package (Kolde & Kolde, 2018), targeting the top 20 species and CAZymes. Alpha diversity was analyzed using *picante* and *vegan* packages to calculate Chao1, Shannon, and Simponeven indices, and bar plots were created with *ggplot2*. Abundance of substrate-specific and total CAZymes, lignin degradation genes, and so forth were presented using scatter, bar, and/or box plots with *ggplot2*. Significantly changed genes in the anaerobic lignin degradation pathway were labeled in red based on *p*-values <.05 with the Kruskal–Wallis test and gene abundances were exhibited by a bar plot using *ggplot2*. C flow changes in the soil microbial community were visualized using radar diagrams for the starch and sucrose metabolism, fatty acid biosynthesis, amino acid metabolism, and nucleotide metabolism pathways from the KEGG database, created with *ggradar* package.

## 3 | RESULTS

### 3.1 | Leaf DOM and soil microbial communities of *S. apetala* and *K. obovata*

#### 3.1.1 | Leaf DOM characteristics

*S. apetala* leaf DOM had 3144 assigned formulas, while *K. obovata* had 2327 formulas (Supplementary File 1). The mass distributions of these formulas (Figure 1a) indicated that *S. apetala* leaf DOM had a lower molecular weight (419.6) compared to *K. obovata* (458.9, Figure 1b). The DOM characteristics analysis revealed that *S. apetala* had higher percentages of lipid (3.69%), protein-like (31.14%), and carbohydrate-like (4.80%) components, and lower percentages of lignin-like (40.97%), tannins (7.67%), aromatic structures (8.65%), and unsaturated hydrocarbons (2.13%) than *K. obovata*. In addition, the C:N mass ratios of *S. apetala* and *K. obovata* leaf DOM were 82.3 and 109.7, respectively (Figure 1b).

#### 3.1.2 | Soil microbial community composition

Microbial diversity analyses revealed lower Chao1 index in tidal flat soil than vegetated soils ($p<.05$, Wilcoxon rank-sum test); but no significant differences were observed among the vegetated soils ($p=.16$, Kruskal–Wallis test, Figure 2A). The Shannon index did not show significant differences ($p=.06$, Figure 2B). Nevertheless, the Simpsoneven index significantly decreased in the vegetated soils compared to tidal flat ($p<.05$, Wilcoxon rank-sum test, Figure 2C), with the lowest value obtained at *K. obovata*. Bacterial community compositions significantly differed between tidal flat and vegetated soils (PERMANOVA, $R^2=.65$, $p<.01$; Anosim, $R^2=.58$, $p<.01$) and were visualized with three distinct clusters (Figure 2D). The top 5 most abundant species were *Deltaproteobacteria bacterium*, *Acidobacteria bacterium*, *Gammaproteobacteria bacterium*, *Chloroflexi bacterium*, and *Proteobacteria bacterium* (Figure 2E). *D. bacterium* was significantly more abundant in *K. obovata* soils compared to the other two groups ($p<.01$, Wilcoxon rank-sum test), accounting for 12.2% of the relative abundance. The decrease in the Simpsoneven index in *K. obovata* soils can be attributed to an increase in *D. bacterium* abundance and a decrease in *P. bacterium* abundance.

#### 3.1.3 | PLFA microbial biomass and its partitioning of assimilated plant-C

The PLFA analysis showed increased microbial biomass after introducing *S. apetala*, but it remained lower than in *K. obovata* soils ($p<.05$, Figure 3A). The total gene abundances of starch and sucrose

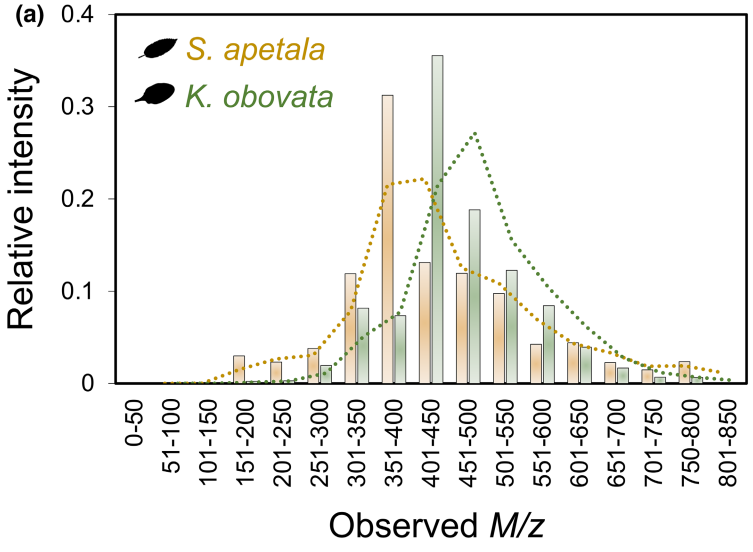


(b)

| Proportion (%) | *S. apetala* | *K. obovata* |
|---|---|---|
| Lipid | 3.69 | 1.59 |
| Protein | 31.14 | 11.09 |
| Carbohydrate | 4.80 | 3.05 |
| Lignin | 40.97 | 50.62 |
| Tannins | 7.67 | 10.44 |
| Others | 11.73 | 23.2 |
| Average Mass | 419.6 | 458.9 |
| C:N mass ratio | 82.3 | 109.7 |

**FIGURE 1** The FT-ICR-MS-based characteristics of leaf DOM from *Sonneratia apetala* and *Kandelia obovata*. The distribution of molecular size (a) and a summary of characteristics (b).

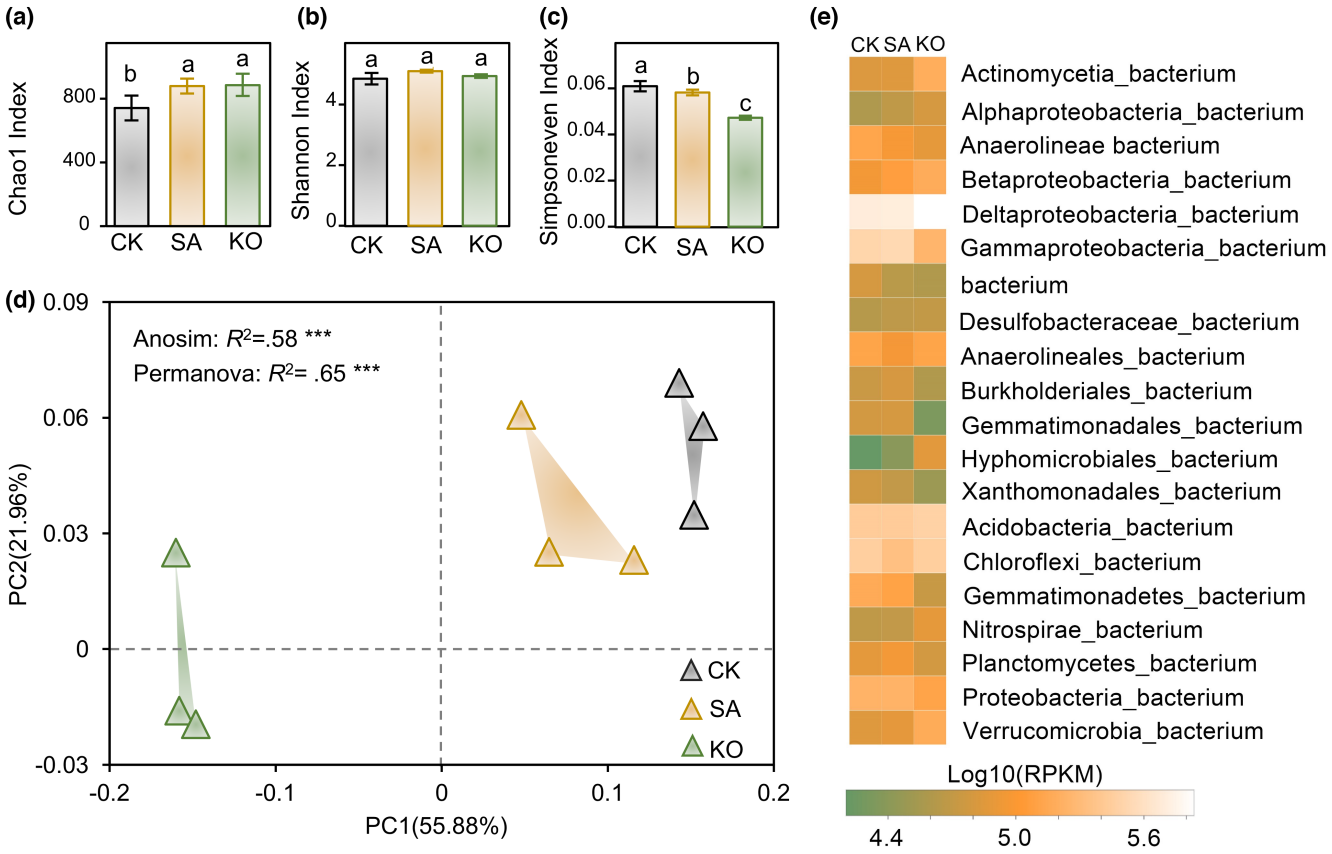


FIGURE 2 The diversity and composition of soil microbial communities. (A)–(C) Differences analyses of alpha-diversity indexes; (D) principal components analysis (PCA), Anosim, and Permanova analyses of the differences of microbial composition based on Brays–Curtis distance; (E) a heatmap showing the abundance of the top 20 species. CK, SA, and KO represent soils sampled from the tidal flat control, *Sonneratia apetala*, and *Kandelia obovata*, respectively.

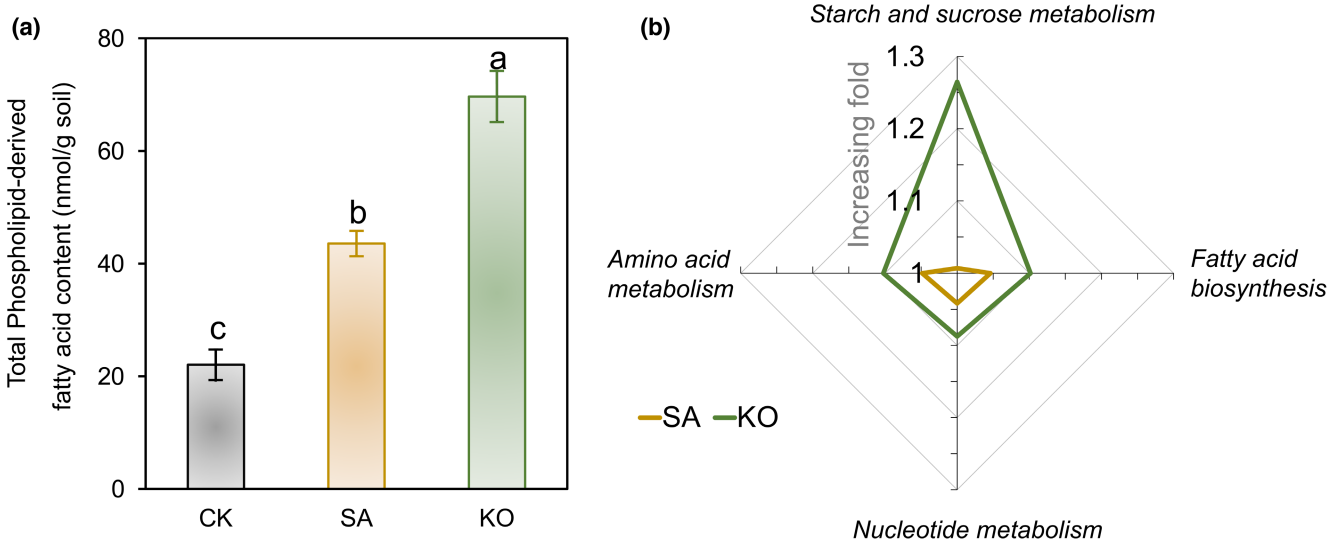


FIGURE 3 Phospholipid fatty acid (PLFA) microbial biomass and its partitioning of assimilated plant-C. (A) The changes in phospholipid-derived fatty acid content, which are presented as means ± SE for $n = 3$; (B) C partitioning in SA and KO soils. CK, SA, and KO represent soils sampled from the tidal flat control, *Sonneratia apetala*, and *Kandelia obovata*, respectively.

metabolism, fatty acid biosynthesis, amino acid metabolism, and nucleotide metabolism were used to calculate the increasing fold, representing their relative abundance in the vegetated mangrove soils versus those in the tidal flat (Figure 3B). *S. apetala* soils had slightly increased potentials for amino acid metabolism, fatty acid biosynthesis, and nucleotide metabolism with 1.048×, 1.046×, and 1.041× higher abundances, respectively, but the potential for starch and sucrose metabolism did not significantly differ (1.006× higher abundance; $p = .51$, Wilcoxon rank-sum test between *S. apetala* and tidal flat soils). In contrast, *K. obovata* soils exhibited significant increases in all pathways (starch and sucrose metabolism, fatty acid biosynthesis, amino acid metabolism, and nucleotide metabolism) compared to the tidal flat soils (all $p$ values <.05). Notably, C flow into the starch and sucrose metabolism pathway increased significantly in *K. obovata* compared to *S. apetala* ($p < .05$).

## 3.2 | The effects of *S. apetala* ages on the plant-litter C degradation

### 3.2.1 | The overall degradation potential of plant-litter C

The overall degradation potential of plant-litter C was assessed by examining the abundance of CAZyme families. A total of 30,925,757 non-redundant genes were obtained from the unassembled mangrove forest soil metagenomes, and 568 CAZy gene families were identified (see Supplementary File 2 for the detailed abundances). Sixty of these CAZy gene families showed significant differences after introducing *S. apetala* ($p < .05$, Kruskal–Wallis test, see Supplementary File 3 for details). The top 50 most abundant CAZy genes were primarily involved in degrading starch, cellulose, hemicellulose, extensin, and lignin (Figure S2A). Although the total abundances of CAZy genes did not significantly differ with the age of *S. apetala* increasing ($p = .058$, df = 2, $\chi^2 = 7.47$, Kruskal–Wallis test, Figure S2B), the relative proportions of the substrate-specific CAZy genes exhibited different patterns (Figure 4). The abundance of genes responsible for degrading starch, hemicellulose, and pectin significantly increased in *S. apetala* soils ($p < .05$, Kruskal–Wallis test).

### 3.2.2 | Aerobic and anaerobic degradation potentials of lignin

The KGEE-based analysis of potential for lignin degradation showed similar trends as CAZymes database (Figure 5A). The gene abundances involved in lignin degradation (including aerobic and anaerobic pathways) did not significantly differ between SA10 and SA20 soils, but both were higher than in the tidal flat soil (both $p$ values <.05, Wilcoxon rank-sum test, Figure 5A). In our metagenomes, we identified all genes matching the lignin aerobic and anaerobic degradation pathways annotated in the KEGG database (Figure 5; Figure S2; Tables S1 and S2). The aerobic lignin degradation pathways showed similar trends, with lower gene abundances in tidal flat soil than in vegetated soils (both $p$ values <.05, Figure 5A). However, the total abundance of 22 anaerobic degradation-associated genes significantly increased with the increasing age of *S. apetala* (Wilcoxon rank-sum test, $p < .05$, SA20 vs. SA10, Figure 5A). Specifically, 7 genes exhibited significant differences during reforestation ($p < .05$, Kruskal–Wallis test, Figure 5B), which were shown in yellow (Figure 5C). The ligases E.C. 6.2.1.25, 6.2.1.27, and 6.2.1.37 responsible for C-S bond formation and the oxidoreductase E.C. 1.1.7.1 increased significantly with the increasing age of *S. apetala* (all $p$ values <.05, Wilcoxon rank-sum test, Figure 5C,D) at the beginning of anaerobic degradation pathway.

## 3.3 | SOC storage and the contribution of plant-derived C and microbial-derived C

The introduction of *S. apetala* significantly enhanced the SOC formation ($p < .01$, Wilcoxon rank-sum test, Figure 6). For example, SOC concentrations of SA10 and SA20 was 19.9% and 18.6% higher,

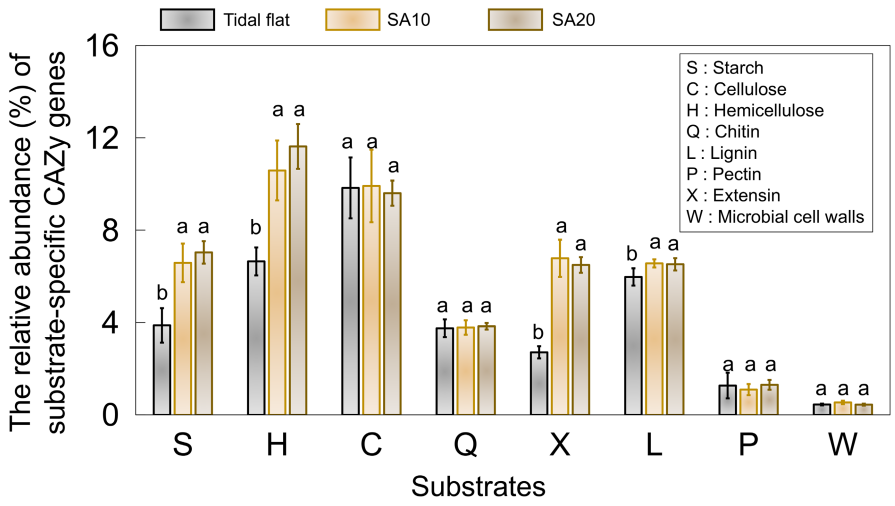


**FIGURE 4** Patterns of substrate-specific degradation potential for plant-derived C in soils with the increasing age of *Sonneratia apetala*. Different letters: Significant difference at $p < .05$ by Wilcoxon rank-sum test for each substrate-specific CAZy gene. SA10 and SA20 represent soils sampled from the 10-year-old and 20-year-old *S. apetala*, respectively.

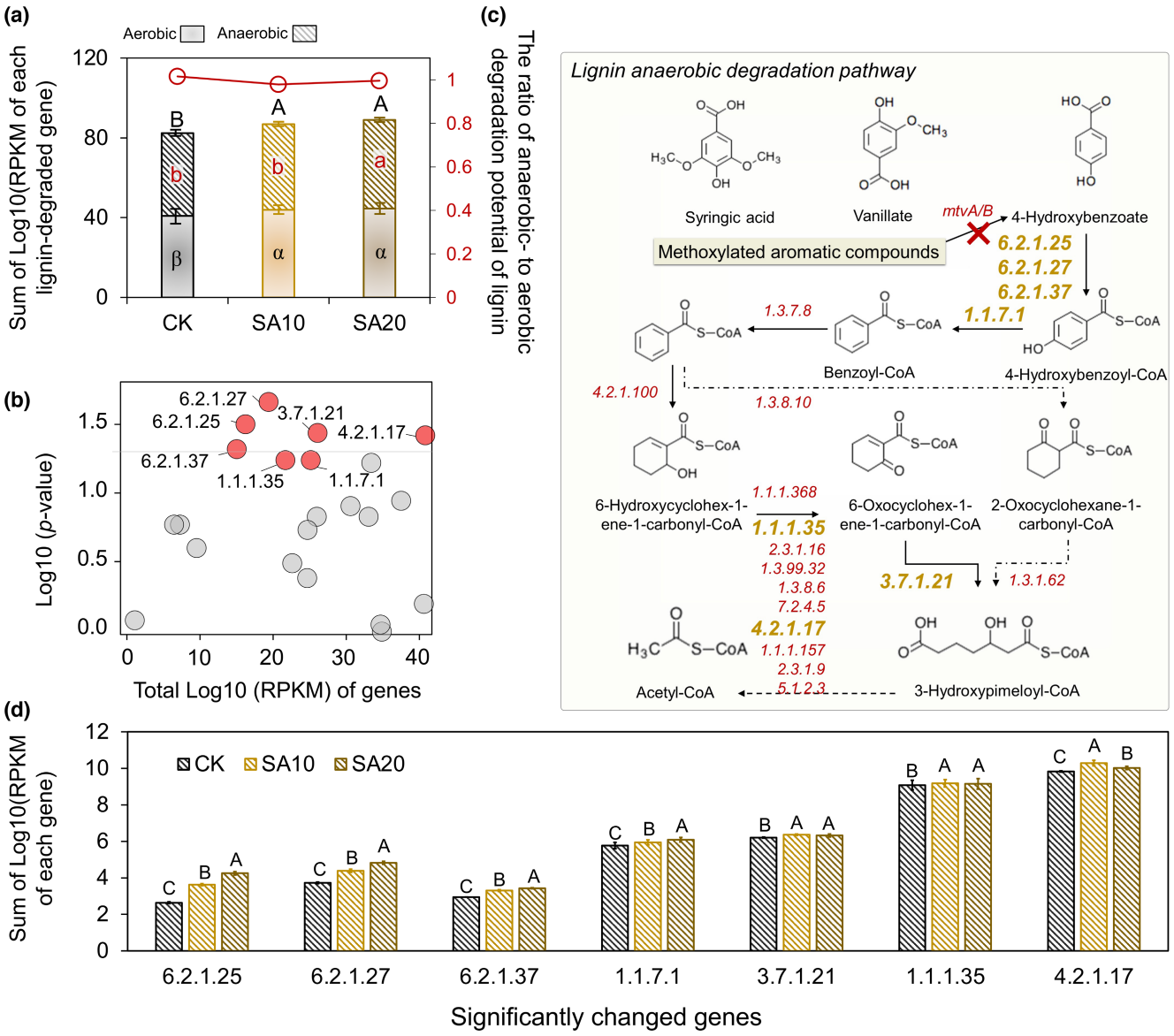


FIGURE 5 Changes of lignin degradation with the increasing age of *Sonneratia apetala*. (A) Comparison of aerobic and anaerobic degradation; (B) a significant difference test (Wilcoxon rank-sum test) used to extract the significant changed genes in lignin anaerobic degradation pathway; (C) the conceptual modes of the anaerobic degradation pathway in the studied mangrove soils and genes with significant and insignificant difference are shown in yellow and red, respectively; (D) changes in the abundance of significant changed genes. Different letters indicate significant differences among groups (Wilcoxon rank-sum test). Values are presented as means ± SE for $n = 3$. SA10 and SA20 represent soils sampled from the 10-year-old and 20-year-old *S. apetala*, respectively.

respectively, compared to tidal flat soil (13.2%). However, the age of *S. apetala* did not significantly affect the SOC concentration ($p = .3$, SA10 vs. SA20). Similarly, the contribution of plant-derived C to SOC was significantly influenced by the introduction of *S. apetala* ($p < .01$), but there were no remarkable changes as mangrove restoration progressed. On average, *S. apetala* communities had approximately 5 times more plant-derived C than tidal flat soil. Nonetheless, the SOC concentration of *S. apetala* (both SA10 and SA20) was significantly lower than in *K. obovata* soil ($p < .01$). Additionally, the contributions of microbial-derived C to SOC in soils vegetated by *S. apetala* were higher than in *K. obovata* soil.

## 4 | DISCUSSION

There is an increasing interest in restoring ecological functions during afforestation. Afforestation not only restores the aboveground vegetation, but also enhances the aboveground-underground ecological relationship by increasing the amount of leaf litter. However, little is known about how leaf litter regulates the microbial-driven transfer of plant-derived C to underlying soil horizons, thereby affecting SOC sequestration during mangrove afforestation. In this study, we investigated changes in FT-ICR-MS-based characteristics of leaf DOM, microbial community diversity and functional potentials

after introducing *S. apetala*, using the tidal flat and the native species as references (Figure 7). Our first hypothesis was supported by the finding that the leaves of *S. apetala* have relatively lower molecular weight and C:N mass ratio compared to *K. obovata*, suggesting that *S. apetala* can release more small-molecule C and nutrients into the soil with the same amount of litterfall. Consequently, the microbial community was dominated by *r*-strategists, which allocated the assimilated plant-derived C into the cell growth, ultimately resulting in a weaker capacity for SOC sequestration in *S. apetala*-vegetated soils. We also clarified whether the age of *S. apetala* affects the degradation of plant-derived C and its contribution to SOC. Our results indicated that the age of *S. apetala* did not significantly influence the degradation potentials of plant-derived C, and thus its contribution of SOC; however, the potentials for anaerobic lignin degradation were significantly elevated in SA20 likely due to the reduced ORP, supporting our second hypothesis. Overall, our study provides valuable insights into the microbial transformation of plant-derived C to SOC during mangrove restoration.

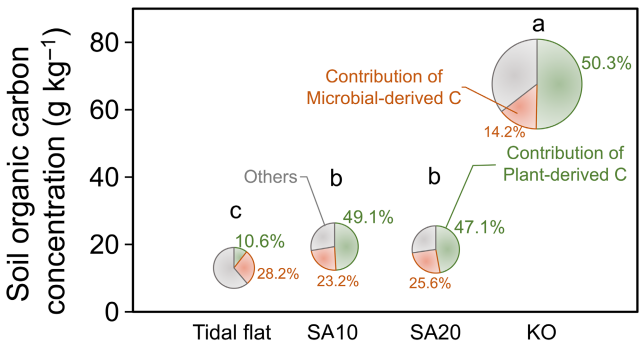


FIGURE 6 Patterns of soil organic carbon and the contribution of plant-derived C (indicated by green color) and microbial-derived C (indicated by orange color). Different letters indicate significant differences in the soil organic carbon concentration among groups (Wilcoxon rank-sum test). SA10, SA20, and KO represent the soils sampled from 10-year-old and 20-year-old *Sonneratia apetala*, and the native mangrove species *Kandelia obovata*.

## 4.1 | Regulation of afforestation on the microbial-driven transfer of C from leaf to blue C pool

Vegetation composition shifts are a key factor dominating changes in C cycling and the formation of the blue C pool during mangrove afforestation (Alongi, 2014; Yang et al., 2016). The C in blue C pools comes primarily from photosynthetically fixed C in autochthonous

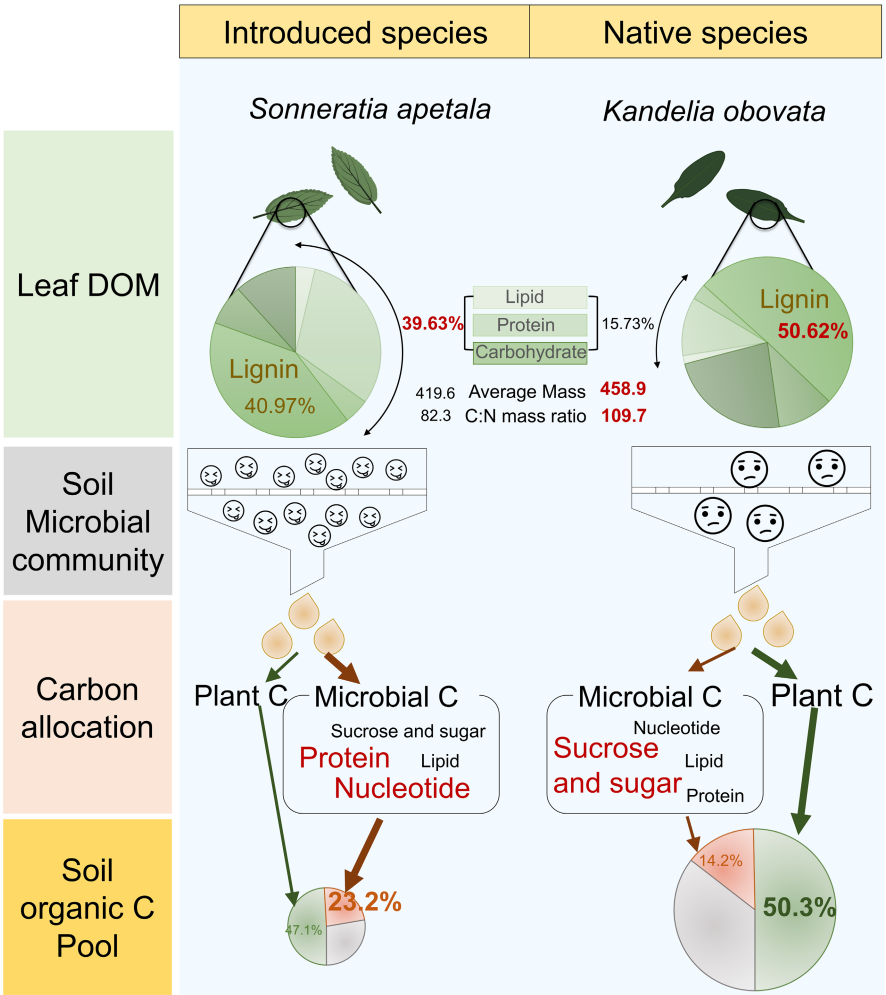


FIGURE 7 A conceptual model showing how afforestation regulates the microbial-driven transfer of carbon from plant litter to the underlying soil horizons in mangroves. The thickness of the arrow indicates the contribution of plant-derived C or microbial-derived C to blue C.

mangrove tree (providing over 50% of the total C sources), with the remainder coming from surrounding terrestrial and marine C (Kristensen et al., 2008). Although previous research has indicated that the relative contribution of terrestrial and marine sources depends on forest location, river flow, and tidal pulse intensity (Krauss et al., 2010; Osland et al., 2012); within the same restoration site, these other factors are relatively consistent. Therefore, the importance of tree species selection becomes more prominent when afforestation. Our study compared the differences between the introduced *S. apetala* and the native *K. obovata* based on the same forest location, tidal timing, and intensity. We demonstrate that the surface SOC concentration in both 10-year-old and 20-year-old *S. apetala* is only one-third of that found in native *K. obovata*. This finding aligns with previous research results (Feng et al., 2019; Lunstrum & Chen, 2014; Yu et al., 2020). Therefore, the selection of tree species is a crucial factor determining the size of the blue C pools during mangrove afforestation.

Mangrove tree species regulate the formation of blue C primarily through leaf litter production (Adame et al., 2021; Kristensen et al., 2008). Although on average about 50% of the average mangrove litterfall is exported from the ecosystem (Adame & Lovelock, 2011); the remaining litterfall still contributes nearly 40% to its total carbon burial (Alongi, 2014; Kristensen et al., 2008). The litterfall triggers a series of soil microbial metabolic activities (Chao et al., 2019; Wang et al., 2014). The quantity and characteristics of leaf litter determine the amount and types of C sources that soil microorganisms can utilize. A long-term observation of litter production of *S. apetala* and *K. obovata* over 10 years revealed that *S. apetala* produces more aboveground biomass and leaf litter compared to *K. obovata* (Liu et al., 2014). Despite the greater quantity of leaf litter from *S. apetala*, the blue C pool remains smaller compared to *K. obovata*. Our findings can provide two explanations:

First, the overall degradation potentials of plant-derived C showed no significant differences between *S. apetala* and *K. obovata*, suggesting a similar transform rate from leaf litter-derived C to SOC pool. Additionally, we observed no significant differences in the extensin-specific decomposition potential were observed between *S. apetala* and *K. obovata* soils. Extensin, a hydroxyproline-rich glycoprotein in the plant cell wall (Camilleri & Ribi, 1986; Lamport et al., 2011), acts as a front-line defense against the breakdown of plant litterfall by microbes (Castilleux et al., 2021). This series of evidence indicates that although there are differences in litter quantity (Liu et al., 2014), the size of the 'valve' regulating the input of litter C into the SOC pool does not significantly differ between *S. apetala* and *K. obovata*. Therefore, the key to clarifying the plant-derived C received by surface soil microbial communities is the characteristics of leaf DOM.

Second, *S. apetala* leaf DOM was characterized by lower molecular weight and C:N mass ratio, and greater amounts of labile nutrients (protein and carbohydrate) than *K. obovata* leaves. After receiving such distinct leaf litter DOM, soil microbial communities exhibited different structures. According to the growth rate hypothesis, fast-growing bacteria (*r*-strategists) require high levels of nucleotides and proteins to support microbial growth and division (Elser et al., 2003; Makino et al., 2003). Our C partitioning analyses supported our hypothesis I, as manifested by the increased nucleotide and amino acid metabolism potentials and decreased starch and sucrose metabolism potentials in the *S. apetala* soils. Therefore, we suggest that the microbial communities in the *S. apetala* soils are primarily dominated by *r-strategists*.

The different growth rates of microbial communities greatly determines their utilization of plant-derived C, thereby explaining the SOC dynamics. *R*-strategists, known for their short lifespan and rapid reproduction under favorable conditions (Hamer & Marschner, 2002; Kuzyakov & Bol, 2006), play a predominant role in decomposing both plant inputs and 'old' SOC when litter releases DOM with a relative low C:N ratio, a phenomenon called the priming effect (Bingeman et al., 1953; Kirkby et al., 2014; Trevathan-Tackett et al., 2018). With this understanding, we propose that in *S. apetala* soils, DOM leaching from the freshly fallen litter enriched in low-molecular-weight C and nutrients, stimulates the growth and dominance of *r*-strategists. Consequently, most of the assimilated plant-derived C is allocated to microbial growth rather than the formation of stabile SOC (Fang et al., 2018; Malik et al., 2020). Therefore, although the mangrove soils (SA10 and SA20) received more fresh litter C than the tidal flats after reforestation, the litter C is likely consumed by microbes and consequently transformed to atmospheric $CO_2$ (Blagodatskaya & Kuzyakov, 2008; Shao et al., 2021). This suggestion well explained our finding that the SOC in SA10 and SA20 topsoil was not highly increased compared to the tidal flat.

Overall, our study sheds light on the role of leaf DOM in shaping structure of soil microbial communities, and emphasizes the significance of microbial community growth strategies in explaining the SOC dynamics during mangrove afforestation. The DOM leaching from *S. apetala* favors the proliferation of *r*-strategists, which rapidly consume C to fuel growth rather than store it. In contrast, the lignin-predominant leaf DOM of *K. obovata* shapes a microbial community dominated by *K*-strategists that grow slower, store the assimilated C in their cells, and ultimately promotes the stabilization and accumulation of SOC. Since parts of these leaf DOMs are exported from mangroves to other blue C ecosystems, such as saltmarshes and seagrasses (Maher et al., 2018; Odum, 1968), the active *S. apetala* leaf DOM may provide a subsidy to nourish adjacent nearshore food webs. However, the contemporary understanding reveals a more intricate scenario that the contribution of mangrove litter to adjacent coastal food webs is limited (Adame et al., 2012). We suggest that it is likely due to the fact that the labile DOM of *S. apetala* leaf is depleted by aquatic microbes as they are tidally exported.

### 4.2 | Age of afforested species enhances the anaerobic degradation potentials for plant-derived C

Lignin constitutes one-fourth of leaf litter and is catabolized through both aerobic and anaerobic degradation (Durante et al., 2018; Levy-Booth et al., 2021). Despite prevalence of anoxic conditions

in mangrove soils, microbial anaerobic lignin degradation remains inadequately understood (Cabral et al., 2018; Durante et al., 2018; Foght, 2008). Our investigation indicates that the potential for anaerobic lignin degradation is equivalent to that for aerobic degradation, highlighting the crucial role of anaerobic lignin degradation in the biospheric cycling of C in mangrove soils. This finding aligns with the study by Benner et al. (1984), which reported highly active anaerobic lignin biodegradation in waterlogged soils. However, we observed an intriguing phenomenon that the potential for anaerobic lignin degradation is enhanced with the progression of mangrove afforestation. Metagenomic analysis further elucidated that 4-hydroxybenzoate-CoA ligase (E.C. 6.2.1.25, 6.2.1.27, 6.2.1.37) were the principal ligase responsible for anaerobic degradation in response to the age of *S. apetala*. This ligase catalyzes the conversion of lignin-based compounds into benzoyl-coenzyme A (benzoyl-CoA), the initial step in the central reductive pathway for aromatic ring degradation under anaerobic conditions (Gibson et al., 1997; Merkel et al., 1989). The regulation of soil enzyme activity by functional genes in microorganisms is a well-established phenomenon (Bahram et al., 2018; Trivedi et al., 2016), and extracellular enzymes play a pivotal role in the decomposition of soil C (Burns et al., 2013). Therefore, the elevated abundance of genes for anaerobic lignin degradation is associated with increased ligase activity, facilitating C anaerobic decomposition. *AadR*, a regulatory gene associated with 4-hydroxybenzoate-CoA ligases, serves as a redox potential sensor (Egland et al., 1997) that activates the expression of this ligase in response to low redox conditions (Egland & Harwood, 2000). As expected, we observed a reduction in the oxidation–reduction potential (ORP) of the topsoil with increasing age of *S.apetala* (Figure S4). This decline in ORP is likely a consequence of the accumulation of perennial leaf litter layers, which inevitably lead to hypoxic topsoil conditions (Huang & Spohn, 2015; Leitner et al., 2016). Thus, the reduced ORP activated *AadR* and the expression of 4-hydroxygenzoate-CoA ligase, thus promoting the potential for anaerobic lignin degradation in the old-aged *S.apetala* soil.

Organic matter, like lignin, settling onto the anoxic sediment acts as an electron source for alternative electron acceptors, such as nitrates and sulfates (Canfield, 1989; Davidova et al., 2007; Evans & Fuchs, 1988; Fernandes et al., 2012). Our study observed that sulfate or nitrate reduction contributed to half of the electron acceptors required for anaerobic reactions, and both anaerobic and aerobic respiration (oxidative phosphorylation pathway) show similar potentials (Figure S5). Additionally, the dominant taxa we observed (*D. bacterium*) is a generalist capable of aerobic and anaerobic lignin degradation, oxidative respiration, and dissimilatory sulfate/nitrate reduction (Figure S6). This highlights *D. bacterium*'s fundamental ability to engage in diverse chemical processes relevant to anaerobic degradation of plant litter, emphasizing the crucial role of anaerobic lignin degradation in mature mangrove soils. Furthermore, anaerobic respiration generates substantial amounts of inorganic reduced compounds, such as sulfur, which contribute to chemoautotrophic C fixation (Gong et al., 2018). Our study found that the C fixation potential of prokaryotes increased with the age of *S. apetala* (Figure S7), suggesting that the growing importance of anaerobic lignin degradation in old-aged mangrove soils may enhance the capacity of the surficial soil to sequester atmospheric $CO_2$ by accelerating C fixation. Given these findings, existing models may underestimate the C sink capacity of mangroves if microbial anaerobic lignin degradation and its possible accompanying $CO_2$ fixation processes are not considered.

## AUTHOR CONTRIBUTIONS

**Zhe Lu:** Conceptualization; data curation; funding acquisition; investigation; methodology; validation; visualization; writing – original draft; writing – review and editing. **Guoming Qin:** Conceptualization; investigation; writing – review and editing. **Shuchai Gan:** Data curation; writing – review and editing. **Hongbin Liu:** Writing – review and editing. **Peter Macreadie:** Funding acquisition; writing – review and editing. **Wee Cheah:** Writing – review and editing. **Faming Wang:** Conceptualization; formal analysis; investigation; methodology; supervision; writing – review and editing.

## ACKNOWLEDGEMENTS

This work was financially supported by the National Natural Science Foundation of China (32301398, U2106209, 32011530164, 32171594, 42007230), ANSO collaborative research (ANSO-CR-KP-2022-11), the CAS Project for Young Scientists in Basic Research (YSBR-037), 2023 Natural Resources Affairs Management-Ecological Forestry Construction Special Project of Forestry Administration of Guangdong Province (2022-8), the CAS Youth Innovation Promotion Association (2021347), the Guangdong Basic and Applied Basic Research Foundation (2021B1515020011, 2021B1212110004, 2023A1515010946), the National Forestry and Grassland Administration Youth Talent Support Program (2020BJ003), the National Key R&D Program of China (2021YFC3100402), Key-Area Research and Development Program of Guangdong Province (2022B1111230001), R & D program of Guangdong Provincial Department of Science and Technology (2018B030324003), South China Botanical Garden, Chinese Academy of Sciences (QNXM-08), and Key laboratory of Vegetation Restoration and Management of Degraded Ecosystems, South China Botanical Garden, Chinese Academy of Sciences (VRMDE2204). PIM thanks the support of an Australian Research Council Discovery Grant (DP200100575).

## CONFLICT OF INTEREST STATEMENT

The authors declare no conflict of interest.

## DATA AVAILABILITY STATEMENT

Data supporting the results in this paper are available via the Supplementary file or archived in institutional repository of South China Botanical Garden, Chinese Academy of Science: https://doi.org/10.57841/casdc.0002902.

## ORCID

*Guoming Qin* https://orcid.org/0000-0002-8959-3118
*Peter I. Macreadie* https://orcid.org/0000-0001-7362-0882
*Faming Wang* https://orcid.org/0000-0002-7543-6779

## REFERENCES


Adame, M. F., Connolly, R. M., Turschwell, M. P., Lovelock, C. E., Fatoyinbo, T., Lagomasino, D., Goldberg, L. A., Holdorf, J., Friess, D. A., Sasmito, S. D., Sanderman, J., Sievers, M., Buelow, C., Kauffman, J. B., Bryan-Brown, D., & Brown, C. J. (2021). Future carbon emissions from global mangrove forest loss. *Global Change Biology*, *27*, 2856–2866. https://doi.org/10.1111/gcb.15656

Adame, M. F., & Lovelock, C. E. (2011). Carbon and nutrient exchange of mangrove forests with the coastal ocean. *Hydrobiologia*, *663*, 23–50. https://doi.org/10.1007/s10750-010-0554-7

Adame, M. F., Wright, S. F., Grinham, A., Lobb, K., Reymond, C. E., & Lovelock, C. E. (2012). Terrestrial–marine connectivity: Patterns of terrestrial soil carbon deposition in coastal sediments determined by analysis of glomalin related soil protein. *Limnology and Oceanography*, *57*, 1492–1502. https://doi.org/10.4319/lo.2012.57.5.1492

Alongi, D. M. (2014). Carbon cycling and storage in mangrove forests. *Annual Review of Marine Science*, *6*, 195–219.

Arndt, S., Jørgensen, B. B., LaRowe, D. E., Middelburg, J. J., Pancost, R. D., & Regnier, P. (2013). Quantifying the degradation of organic matter in marine sediments: A review and synthesis. *Earth-Science Reviews*, *123*, 53–86. https://doi.org/10.1016/j.earscirev.2013.02.008

Bahram, M., Hildebrand, F., Forslund, S. K., Anderson, J. L., Soudzilovskaia, N. A., Bodegom, P. M., Bengtsson-Palme, J., Anslan, S., Coelho, L. P., & Harend, H. (2018). Structure and function of the global topsoil microbiome. *Nature*, *560*, 233–237. https://doi.org/10.1038/s41586-018-0386-6

Bardgett, R. D., Lovell, R. D., Hobbs, P. J., & Jarvis, S. C. (1999). Seasonal changes in soil microbial communities along a fertility gradient of temperate grasslands. *Soil Biology and Biochemistry*, *31*(8), 1021–1030. https://doi.org/10.1016/S0038-0717(99)00019-6

Bardgett, R. D., & van der Putten, W. H. (2014). Belowground biodiversity and ecosystem functioning. *Nature*, *515*(7528), 505–511. https://doi.org/10.1038/nature13855

Benner, R., Maccubbin, A., & Hodson, R. E. (1984). Anaerobic biodegradation of the lignin and polysaccharide components of lignocellulose and synthetic lignin by sediment microflora. *Applied and Environmental Microbiology*, *47*(5), 998–1004. https://doi.org/10.1128/AEM.47.5.998-1004.1984

Bertram, C., Quaas, M., Reusch, T. B. H., Vafeidis, A. T., Wolff, C., & Rickels, W. (2021). The blue carbon wealth of nations. *Nature Climate Change*, *11*, 704–709. https://doi.org/10.1038/s41558-021-01073-2

Bingeman, C. W., Varner, J., & Martin, W. (1953). The effect of the addition of organic materials on the decomposition of an organic soil. *Soil Science Society of America Journal*, *17*(1), 34–38. https://doi.org/10.2136/sssaj1953.03615995001700010008x

Blackburn, J. W. T., Kew, W., Graham, M. C., & Uhrín, D. (2017). Laser desorption/ionization coupled to FTICR mass spectrometry for studies of natural organic matter. *Analytical Chemistry*, *89*, 4382–4386. https://doi.org/10.1021/acs.analchem.6b04555

Blagodatskaya, E., & Kuzyakov, Y. (2008). Mechanisms of real and apparent priming effects and their dependence on soil microbial biomass and community structure: Critical review. *Biology and Fertility of Soils*, *45*(2), 115–131. https://doi.org/10.1007/s00374-008-0334-y

Bossio, D. A., Fleck, J. A., Scow, K. M., & Fujii, R. (2006). Alteration of soil microbial communities and water quality in restored wetlands. *Soil Biology and Biochemistry*, *38*(7), 1223–1233. https://doi.org/10.1016/j.soilbio.2005.09.011

Buchfink, B., Xie, C., & Huson, D. H. (2015). Fast and sensitive protein alignment using DIAMOND. *Nature Methods*, *12*(1), 59–60. https://doi.org/10.1038/nmeth.3176

Burns, R. G., DeForest, J. L., Marxsen, J., Sinsabaugh, R. L., Stromberger, M., Wallenstein, E. M. D., Weintraub, M. N., & Zoppini, A. (2013). Soil enzymes in a changing environment: Current knowledge and future directions. *Soil Biology and Biochemistry*, *58*, 216–234. https://doi.org/10.1016/j.soilbio.2012.11.009

Cabral, L., Pereira de Sousa, S. T., Júnior, G. V. L., Hawley, E., Andreote, F. D., Hess, M., & de Oliveira, V. M. (2018). Microbial functional responses to long-term anthropogenic impact in mangrove soils. *Ecotoxicology and Environmental Safety*, *160*, 231–239. https://doi.org/10.1016/j.ecoenv.2018.05.050

Camilleri, J. C., & Ribi, G. (1986). Leaching of dissolved organic carbon (DOC) from dead leaves, formation of flakes from DOC, and feeding on flakes by crustaceans in mangroves. *Marine Biology*, *91*, 337–344. https://doi.org/10.1007/BF00428591

Canfield, D. E. (1989). Sulfate reduction and oxic respiration in marine sediments: Implications for organic carbon preservation in euxinic environments. *Deep Sea Research Part A. Oceanographic Research Papers*, *36*, 121–138. https://doi.org/10.1016/0198-0149(89)90078-5

Cantarel, B. L., Coutinho, P. M., Rancurel, C., Bernard, T., Lombard, V., & Henrissat, B. (2009). The carbohydrate-active EnZymes database (CAZy): An expert resource for glycogenomics. *Nucleic Acids Research*, *37*(Database issue), D233–D238. https://doi.org/10.1093/nar/gkn663

Canuel, E. A., & Hardison, A. K. (2016). Sources, ages, and alteration of organic matter in estuaries. *Annual Review of Marine Science*, *8*, 409–434. https://doi.org/10.1146/annurev-marine-122414-034053

Castilleux, R., Plancot, B., Vicré, M., Nguema-Ona, E., & Driouich, A. (2021). Extensin, an underestimated key component of cell wall defence? *Annals of Botany*, *127*(4), 709–713. https://doi.org/10.1093/aob/mcaa198

Chao, L., Liu, Y., Freschet, G. T., Zhang, W., Yu, X., Zheng, W., Guan, X., Yang, Q., Chen, L., & Dijkstra, F. A. (2019). Litter carbon and nutrient chemistry control the magnitude of soil priming effect. *Functional Ecology*, *33*(5), 876–888. https://doi.org/10.1111/1365-2435.13320

Chen, H., Liao, B., Peng, C., Zhang, Y., Guan, W., & Yang, G. (2014). Eradicating invasive *Spartina alterniflora* with alien *Sonneratia apetala* and its implications for invasion controls. *Ecological Engineering*, *73*, 367–372. https://doi.org/10.1016/j.ecoleng.2014.09.020

Chen, Y., Chen, G., Robinson, D., Yang, Z., Guo, J., Xie, J., Fu, S., Zhou, L., & Yang, Y. (2016). Large amounts of easily decomposable carbon stored in subtropical forest subsoil are associated with *r*-strategy-dominated soil microbes. *Soil Biology and Biochemistry*, *95*, 233–242. https://doi.org/10.1016/j.soilbio.2015.12.011

Cotrufo, M. F., Wallenstein, M. D., Boot, C. M., Denef, K., & Paul, E. (2013). The microbial efficiency-matrix stabilization (MEMS) framework integrates plant litter decomposition with soil organic matter stabilization: Do labile plant inputs form stable soil organic matter? *Global Change Biology*, *19*, 988–995. https://doi.org/10.1111/gcb.12113

Davidova, I. A., Gieg, L. M., Duncan, K. E., & Suflita, J. M. (2007). Anaerobic phenanthrene mineralization by a carboxylating sulfate-reducing bacterial enrichment. *The ISME Journal*, *1*, 436–442. https://doi.org/10.1038/ismej.2007.59

Dignac, M.-F., Bahri, H., Rumpel, C., Rasse, D., Bardoux, G., Balesdent, J., Girardin, C., Chenu, C., & Mariotti, A. (2005). Carbon-13 natural abundance as a tool to study the dynamics of lignin monomers in soil: An appraisal at the Closeaux experimental field (France). *Geoderma*, *128*, 3–17. https://doi.org/10.1016/j.geoderma.2004.12.011

Dittmar, T., Koch, B., Hertkorn, N., & Kattner, G. (2008). A simple and efficient method for the solid-phase extraction of dissolved organic matter (SPE-DOM) from seawater. *Limnology and*

*Oceanography: Methods*, *6*, 230–235. https://doi.org/10.4319/lom.2008.6.230

Dittmar, T., & Lara, R. (2001). Driving forces behind nutrient and organic matter dynamics in a mangrove tidal creek in North Brazil. *Estuarine, Coastal and Shelf Science*, *52*, 249–259. https://doi.org/10.1006/ecss.2000.0749

Donato, D. C., Kauffman, J. B., Murdiyarso, D., Kurnianto, S., Stidham, M., & Kanninen, M. (2011). Mangroves among the most carbon-rich forests in the tropics. *Nature Geoscience*, *4*, 293–297. https://doi.org/10.1038/ngeo1123

Dungait, J. A., Hopkins, D. W., Gregory, A. S., & Whitmore, A. P. (2012). Soil organic matter turnover is governed by accessibility not recalcitrance. *Global Change Biology*, *18*, 1781–1796. https://doi.org/10.1111/j.1365-2486.2012.02665.x

Durante, G., Gómez Álvarez, H., Blázquez, B., Fernández Llamosas, H., Martín-Moldes, Z., Sanz, D., Nogales, J., Carmona, M., & Díaz, E. (2018). Anaerobic pathways for the catabolism of aromatic compounds. In M. Carmona & E. Díaz (Eds.), *Microbial catabolism of xenobiotic compounds* (pp. 333–390). Springer. https://doi.org/10.1007/82_2018_108

Egland, P. G., & Harwood, C. S. (2000). HbaR, a 4-hydroxybenzoate sensor and FNR-CRP superfamily member, regulates anaerobic 4-hydroxybenzoate degradation by *Rhodopseudomonas palustris*. *Journal of Bacteriology*, *182*, 100–106. https://doi.org/10.1128/JB.182.1.100-106.2000

Egland, P. G., Pelletier, D. A., Dispensa, M., Gibson, J., & Harwood, C. S. (1997). A cluster of bacterial genes for anaerobic benzene ring biodegradation. *Journal of Bacteriology*, *179*, 6484–6489. https://doi.org/10.1128/jb.179.20.6484-6489.1997

Elser, J. J., Acharya, K., Kyle, M., Cotner, J., Makino, W., Markow, T., Watts, T., Hobbie, S., Fagan, W., Schade, J., Hood, J., & Sterner, R. W. (2003). Growth rate–stoichiometry couplings in diverse biota. *Ecology Letters*, *6*, 936–943. https://doi.org/10.1046/j.1461-0248.2003.00518.x

Evans, W. C., & Fuchs, G. (1988). Anaerobic degradation of aromatic compounds. *Annual Reviews in Microbiology*, *42*, 289–317. https://doi.org/10.1146/annurev.mi.42.100188.001445

Fang, Y., Nazaries, L., Singh, B. K., & Singh, B. P. (2018). Microbial mechanisms of carbon priming effects revealed during the interaction of crop residue and nutrient inputs in contrasting soils. *Global Change Biology*, *24*, 2775–2790. https://doi.org/10.1111/gcb.14008

Feng, J., Wang, S., Wang, S., Ying, R., Yin, F., Jiang, L., & Li, Z. (2019). Effects of invasive *Spartina alterniflora* Loisel. And subsequent ecological replacement by *Sonneratia apetala* Buch.-Ham. on soil organic carbon fractions and stock. *Forests*, *10*, 171. https://doi.org/10.3390/f10020171

Fernandes, S. O., Michotey, V. D., Guasco, S., Bonin, P. C., & Bharathi, P. A. (2012). Denitrification prevails over anammox in tropical mangrove sediments (Goa, India). *Marine Environmental Research*, *74*, 9–19. https://doi.org/10.1016/j.marenvres.2011.10.005

Foght, J. (2008). Anaerobic biodegradation of aromatic hydrocarbons: Pathways and prospects. *Microbial Physiology*, *15*, 93–120. https://doi.org/10.1007/s10295-007-0298-4

Frostegård, Å., Tunlid, A., & Bååth, E. (2011). Use and misuse of PLFA measurements in soils. *Soil Biology and Biochemistry*, *43*, 1621–1625. https://doi.org/10.1016/j.soilbio.2011.01.005

Frostegård, A., & Bååth, E. (1996). Use of phospholipid fatty acid analysis to estimate bacterial and fungal biomass in soil. *Biology and Fertility of Soils*, *22*, 59–65. http://doi.org.10.1007/BF00384433

Gan, S., Guo, P., Wu, Y., & Zhao, Y. (2021). A novel method for unraveling the black box of dissolved organic matter in soils by FT-ICR-MS coupled with induction-based nanospray ionization. *Environmental Science & Technology Letters*, *8*, 356–361. https://doi.org/10.1021/acs.estlett.1c00246

Gibson, J., Dispensa, M., & Harwood, C. S. (1997). 4-hydroxybenzoyl coenzyme a reductase (dehydroxylating) is required for anaerobic degradation of 4-hydroxybenzoate by *Rhodopseudomonas palustris* and shares features with molybdenum-containing hydroxylases. *Journal of Bacteriology*, *179*, 634–642. https://doi.org/10.1128/jb.179.3.634-642.1997

Gong, F., Zhu, H., Zhang, Y., & Li, Y. (2018). Biological carbon fixation: From natural to synthetic. *Journal of $CO_2$ Utilization*, *28*, 221–227. https://doi.org/10.1016/j.jcou.2018.07.022

Hamer, U., & Marschner, B. (2002). Priming effects of sugars, amino acids, organic acids and catechol on the mineralization of lignin and peat. *Journal of Plant Nutrition and Soil Science*, *165*, 261–268. https://doi.org/10.1002/1522-2624(200206)165:3<261::AID-JPLN261>3.0.CO;2-U

Hedges, J. I., & Ertel, J. R. (1982). Characterization of lignin by gas capillary chromatography of cupric oxide oxidation products. *Analytical Chemistry*, *54*, 174–178. https://doi.org/10.1021/ac00239a007

Hiraishi, T., Krug, T., Tanabe, K., Srivastava, N., Baasansuren, J., Fukuda, M., & Troxler, T. (2014). *2013 supplement to the 2006 IPCC guidelines for national greenhouse gas inventories: Wetlands*. IPCC. https://doi.org/10.1017/CBO9781107415324

Huang, W., & Spohn, M. (2015). Effects of long-term litter manipulation on soil carbon, nitrogen, and phosphorus in a temperate deciduous forest. *Soil Biology and Biochemistry*, *83*, 12–18. https://doi.org/10.1016/j.soilbio.2015.01.010

Hur, J., Park, M.-H., & Schlautman, M. A. (2009). Microbial transformation of dissolved leaf litter organic matter and its effects on selected organic matter operational descriptors. *Environmental Science & Technology*, *43*, 2315–2321. https://doi.org/10.1021/es802828u

Indorf, C., Dyckmans, J., Khan, K. S., & Joergensen, R. G. (2011). Optimisation of amino sugar quantification by HPLC in soil and plant hydrolysates. *Biology and Fertility of Soils*, *47*, 387–396. https://doi.org/10.1007/s00374-011-0555-5

Kirkby, C. A., Richardson, A. E., Wade, L. J., Passioura, J. B., Batten, G. D., Blanchard, C., & Kirkegaard, J. A. (2014). Nutrient availability limits carbon sequestration in arable soils. *Soil Biology and Biochemistry*, *68*, 402–409. https://doi.org/10.1016/j.soilbio.2013.10.014

Kolde, R., & Kolde, M. R. (2018). Package '*pheatmap*'. R Package 1. CRAN.R-project.org/package=pheatmap

Kramer, M. G., Lajtha, K., & Aufdenkampe, A. K. (2017). Depth trends of soil organic matter C:N and $^{15}N$ natural abundance controlled by association with minerals. *Biogeochemistry*, *136*, 237–248. https://doi.org/10.1007/s10533-017-0378-x

Krauss, K. W., Cahoon, D. R., Allen, J. A., Ewel, K. C., Lynch, J. C., & Cormier, N. (2010). Surface elevation change and susceptibility of different mangrove zones to sea-level rise on Pacific high islands of Micronesia. *Ecosystems*, *13*, 129–143. https://doi.org/10.1007/s10021-009-9307-8

Kristensen, E., Bouillon, S., Dittmar, T., & Marchand, C. (2008). Organic carbon dynamics in mangrove ecosystems: A review. *Aquatic Botany*, *89*, 201–219. https://doi.org/10.1016/j.aquabot.2007.12.005

Kuzyakov, Y., & Bol, R. (2006). Sources and mechanisms of priming effect induced in two grassland soils amended with slurry and sugar. *Soil Biology and Biochemistry*, *38*, 747–758. https://doi.org/10.1016/j.soilbio.2005.07.007

Lamport, D. T., Kieliszewski, M. J., Chen, Y., & Cannon, M. C. (2011). Role of the extensin superfamily in primary cell wall architecture. *Plant Physiology*, *156*, 11–19. https://doi.org/10.1104/pp.110.169011

Leadbeater, D. R., Oates, N. C., Bennett, J. P., Li, Y., Dowle, A. A., Taylor, J. D., Alponti, J. S., Setchfield, A. T., Alessi, A. M., Helgason, T., McQueen-Mason, S. J., & Bruce, N. C. (2021). Mechanistic

strategies of microbial communities regulating lignocellulose deconstruction in a UK salt marsh. *Microbiome*, *9*, 48. https://doi.org/10.1186/s40168-021-01011-5

Leitner, S., Sae-Tun, O., Kranzinger, L., Zechmeister-Boltenstern, S., & Zimmermann, M. (2016). Contribution of litter layer to soil greenhouse gas emissions in a temperate beech forest. *Plant and Soil*, *403*, 455–469. https://doi.org/10.1007/s11104-016-2845-1

Levy-Booth, D. J., Hashimi, A., Roccor, R., Liu, L.-Y., Renneckar, S., Eltis, L. D., & Mohn, W. W. (2021). Genomics and metatranscriptomics of biogeochemical cycling and degradation of lignin-derived aromatic compounds in thermal swamp sediment. *The ISME Journal*, *15*, 879–893. https://doi.org/10.1038/s41396-020-00822-5

Liang, C. (2020). Soil microbial carbon pump: Mechanism and appraisal. *Soil Ecology Letters*, *2*, 241–254. https://doi.org/10.1007/s42832-020-00036-5

Liang, C., Amelung, W., Lehmann, J., & Kästner, M. (2019). Quantitative assessment of microbial necromass contribution to soil organic matter. *Global Change Biology*, *25*, 3578–3590. https://doi.org/10.1111/gcb.14762

Liang, C., Schimel, J. P., & Jastrow, J. D. (2017). The importance of anabolism in microbial control over soil carbon storage. *Nature Microbiology*, *2*, 1–6. https://doi.org/10.1038/s41564-016-0059-9

Liu, L., Li, F., Yang, Q., Tam, N. F., Liao, W., & Zan, Q. (2014). Long-term differences in annual litter production between alien (*Sonneratia apetala*) and native (*Kandelia obovata*) mangrove species in Futian, Shenzhen, China. *Marine Pollution Bulletin*, *85*, 747–753. https://doi.org/10.1016/j.marpolbul.2014.04.047

Lunstrum, A., & Chen, L. (2014). Soil carbon stocks and accumulation in young mangrove forests. *Soil Biology and Biochemistry*, *75*, 223–232. https://doi.org/10.1016/j.soilbio.2014.04.008

Ma, T., Zhu, S., Wang, Z., Chen, D., Dai, G., Feng, B., Su, X., Hu, H., Li, K., & Han, W. (2018). Divergent accumulation of microbial necromass and plant lignin components in grassland soils. *Nature Communications*, *9*, 3480. https://doi.org/10.1038/s41467-018-05959-4

Macreadie, P. I., Anton, A., Raven, J. A., Beaumont, N., Connolly, R. M., Friess, D. A., Kelleway, J. J., Kennedy, H., Kuwae, T., & Lavery, P. S. (2019). The future of blue carbon science. *Nature Communications*, *10*, 3998. https://doi.org/10.1038/s41467-019-11693-w

Macreadie, P. I., Costa, M. D. P., Atwood, T. B., Friess, D. A., Kelleway, J. J., Kennedy, H., Lovelock, C. E., Serrano, O., & Duarte, C. M. (2021). Blue carbon as a natural climate solution. *Nature Reviews Earth and Environment*, *2*, 826–839. https://doi.org/10.1038/s43017-021-00209-1

Maher, D. T., Call, M., Santos, I. R., & Sanders, C. J. (2018). Beyond burial: Lateral exchange is a significant atmospheric carbon sink in mangrove forests. *Biology Letters*, *14*, 20180200. https://doi.org/10.1098/rsbl.2018.0200

Makino, W., Cotner, J., Sterner, R., & Elser, J. (2003). Are bacteria more like plants or animals? Growth rate and resource dependence of bacterial C:N:P stoichiometry. *Functional Ecology*, *17*, 121–130. https://doi.org/10.1046/j.1365-2435.2003.00700.x

Malik, A. A., Martiny, J. B., Brodie, E. L., Martiny, A. C., Treseder, K. K., & Allison, S. D. (2020). Defining trait-based microbial strategies with consequences for soil carbon cycling under climate change. *The ISME Journal*, *14*, 1–9. https://doi.org/10.1038/s41396-020-00789-8

Mambelli, S., Bird, J. A., Gleixner, G., Dawson, T. E., & Torn, M. S. (2011). Relative contribution of foliar and fine root pine litter to the molecular composition of soil organic matter after in situ degradation. *Organic Geochemistry*, *42*, 1099–1108. https://doi.org/10.1016/j.orggeochem.2011.07.008

Marchand, C., Disnar, J. R., Lallier-Vergès, E., & Lottier, N. (2005). Early diagenesis of carbohydrates and lignin in mangrove sediments subject to variable redox conditions (French Guiana). *Geochimica et Cosmochimica Acta*, *69*, 131–142. https://doi.org/10.1016/j.gca.2004.06.035

Marschner, B., Brodowski, S., Dreves, A., Gleixner, G., Gude, A., Grootes, P. M., Hamer, U., Heim, A., Jandl, G., & Ji, R. (2008). How relevant is recalcitrance for the stabilization of organic matter in soils? *Journal of Plant Nutrition and Soil Science*, *171*, 91–110. https://doi.org/10.1002/jpln.200700049

Merkel, S. M., Eberhard, A., Gibson, J., & Harwood, C. (1989). Involvement of coenzyme A thioesters in anaerobic metabolism of 4-hydroxybenzoate by *Rhodopseudomonas palustris*. *Journal of Bacteriology*, *171*, 1–7. https://doi.org/10.1128/jb.171.1.1-7.1989

Odum, E. P. (1968). A research challenge: Evaluating the productivity of coastal and estuarine water. *Proceedings of the second sea grant conference*, pp. 63–64. University of Rhode Island, Newport, RI.

Osland, M. J., Spivak, A. C., Nestlerode, J. A., Lessmann, J. M., Almario, A. E., Heitmuller, P. T., Russell, M. J., Krauss, K. W., Alvarez, F., & Dantin, D. D. (2012). Ecosystem development after mangrove wetland creation: Plant–soil change across a 20-year chronosequence. *Ecosystems*, *15*, 848–866. https://doi.org/10.1007/s10021-012-9551-1

Prosser, J., Bohannon, B., Curtis, T., Ellis, R., Firestone, M., Freckleton, R., Green, J., Green, L., Killham, K., & Lennon, J. (2007). The role of ecological theory in microbiology. *Nature Reviews Microbiology*, *5*(5), 384. https://doi.org/10.1038/nrmicro1643

R Development Core Team (2009). R: A language and environment for statistical computing. R foundation for statistical computing: Vienna, Austria. *Computing*, *14*, 12–21. https://doi.org.10.1890/0012-9658(2002)083[3097:CFHIWS]2.0.CO;2

Rao, M. N., Ganguly, D., Prasad, M., Singh, G., Purvaja, R., Biswal, M., & Ramesh, R. (2021). Interspecific variations in mangrove stem biomass: A potential storehouse of sequestered carbon. *Regional Studies in Marine Science*, *48*, 102044. https://doi.org/10.1016/j.rsma.2021.102044

Ren, H., Chen, H., Li, Z. A., & Han, W. (2010). Biomass accumulation and carbon storage of four different aged *Sonneratia apetala* plantations in southern China. *Plant and Soil*, *327*, 279–291. https://doi.org/10.1007/s11104-009-0041-1

Ren, H., Jian, S., Lu, H., Zhang, Q., Shen, W., Han, W., Yin, Z., & Guo, Q. (2008). Restoration of mangrove plantations and colonisation by native species in Leizhou bay, South China. *Ecological Research*, *23*, 401–407. https://doi.org/10.1007/s11284-007-0368-7

Ren, H., Lu, H., Shen, W., Huang, C., Guo, Q., & Jian, S. (2009). *Sonneratia apetala* Buch. Ham in the mangrove ecosystems of China: An invasive species or restoration species? *Ecological Engineering*, *35*, 1243–1248. https://doi.org/10.1016/j.ecoleng.2009.03.013

Robertson, S. A., Mason, S. L., Hack, E., & Abbott, G. D. (2008). A comparison of lignin oxidation, enzymatic activity and fungal growth during white-rot decay of wheat straw. *Organic Geochemistry*, *39*, 945–951. https://doi.org/10.1016/j.orggeochem.2008.03.008

Sanders-DeMott, R., Eagle, M. J., Kroeger, K. D., Wang, F., Brooks, T. W., O'Keefe Suttles, J. A., Nick, S. K., Mann, A. G., & Tang, J. (2022). Impoundment increases methane emissions in *Phragmites*-invaded coastal wetlands. *Global Change Biology*, *28*, 4539–4557. https://doi.org/10.1111/gcb.16096

Sayer, E. J. (2006). Using experimental manipulation to assess the roles of leaf litter in the functioning of forest ecosystems. *Biological Reviews*, *81*, 1–31. https://doi.org/10.1017/S1464793105006949

Schneckenberger, K., Demin, D., Stahr, K., & Kuzyakov, Y. (2008). Microbial utilization and mineralization of [$^{14}$C] glucose added in six orders of concentration to soil. *Soil Biology and Biochemistry*, *40*, 1981–1988. https://doi.org/10.1016/j.soilbio.2008.03.027

Shao, P., Lynch, L., Xie, H., Bao, X., & Liang, C. (2021). Tradeoffs among microbial life history strategies influence the fate of microbial residues in subtropical forest soils. *Soil Biology and Biochemistry*, *153*, 108112. https://doi.org/10.1016/j.soilbio.2021.108112

Soares, M. L. G., & Schaeffer-Novelli, Y. (2005). Above-ground biomass of mangrove species. I. Analysis of models. *Estuarine, Coastal and Shelf Science*, *65*, 1–18. https://doi.org/10.1016/j.ecss.2005.05.032

Trevathan-Tackett, S. M., Thomson, A. C., Ralph, P. J., & Macreadie, P. I. (2018). Fresh carbon inputs to seagrass sediments induce variable microbial priming responses. *Science of the Total Environment*, *621*, 663–669. https://doi.org/10.1016/j.scitotenv.2017.11.193

Trivedi, P., Delgado-Baquerizo, M., Trivedi, C., Hu, H., Anderson, I. C., Jeffries, T. C., Zhou, J., & Singh, B. K. (2016). Microbial regulation of the soil carbon cycle: Evidence from gene–enzyme relationships. *The ISME Journal*, *10*, 2593–2604. https://doi.org/10.1038/ismej.2016.65

Tunlid, A., Hoitink, H., Low, C., & White, D. (1989). Characterization of bacteria that suppress Rhizoctonia damping-off in bark compost media by analysis of fatty acid biomarkers. *Applied and Environmental Microbiology*, *55*, 1368–1374. https://doi.org/10.1128/AEM.55.6.1368-1374.1989

Wang, F., Eagle, M., Kroeger, K. D., Spivak, A. C., & Tang, J. (2021). Plant biomass and rates of carbon dioxide uptake are enhanced by successful restoration of tidal connectivity in salt marshes. *Science of the Total Environment*, *750*, 141566. https://doi.org/10.1016/j.scitotenv.2020.141566

Wang, F., Liu, J., Qin, G., Zhang, J., Zhou, J., Wu, J., Zhang, L., Thapa, P., Sanders, C. J., Santos, I. R., Li, X., Lin, G., Weng, Q., Tang, J., Jiao, N., & Ren, H. (2023). Coastal blue carbon in China as a nature-based solution toward carbon neutrality. *The Innovation*, *4*, 100481. https://doi.org/10.1016/j.xinn.2023.100481

Wang, F., Sanders, C. J., Santos, I. R., Tang, J., Schuerch, M., Kirwan, M. L., Kopp, R. E., Zhu, K., Li, X., Yuan, J., Liu, W., & Li, Z. A. (2020). Global blue carbon accumulation in tidal wetlands increases with climate change. *National Science Review*, *8*, nwaa296. https://doi.org/10.1093/nsr/nwaa296

Wang, Q., Wang, S., He, T., Liu, L., & Wu, J. (2014). Response of organic carbon mineralization and microbial community to leaf litter and nutrient additions in subtropical forest soils. *Soil Biology and Biochemistry*, *71*, 13–20. https://doi.org/10.1016/j.soilbio.2014.01.017

Xu, S., Liu, L., & Sayer, E. J. (2013). Variability of above-ground litter inputs alters soil physicochemical and biological processes: A meta-analysis of litterfall-manipulation experiments. *Biogeosciences*, *10*, 7423–7433. https://doi.org/10.5194/bg-10-7423-2013

Yang, W., An, S., Zhao, H., Xu, L., Qiao, Y., & Cheng, X. (2016). Impacts of *Spartina alterniflora* invasion on soil organic carbon and nitrogen pools sizes, stability, and turnover in a coastal salt marsh of eastern China. *Ecological Engineering*, *86*, 174–182. https://doi.org/10.1016/j.ecoleng.2015.11.010

Yang, Z., Song, W., Zhao, Y., Zhou, J., Wang, Z., Luo, Y., Li, Y., & Lin, G. (2018). Differential responses of litter decomposition to regional excessive nitrogen input and global warming between two mangrove species. *Estuarine, Coastal and Shelf Science*, *214*, 141–148. https://doi.org/10.1016/j.ecss.2018.09.009

Yu, C., Feng, J., Liu, K., Wang, G., Zhu, Y., Chen, H., & Guan, D. (2020). Changes of ecosystem carbon stock following the plantation of exotic mangrove *Sonneratia apetala* in Qi'ao Island, China. *Science of the Total Environment*, *717*, 137142. https://doi.org/10.1016/j.scitotenv.2020.137142

Yu, T., Wu, W., Liang, W., Lever, M. A., Hinrichs, K. U., & Wang, F. (2018). Growth of sedimentary Bathyarchaeota on lignin as an energy source. *Proceedings of the National Academy of Sciences of the United States of America*, *115*, 6022–6027. https://doi.org/10.1073/pnas.1801074215

## SUPPORTING INFORMATION

Additional supporting information can be found online in the Supporting Information section at the end of this article.

**How to cite this article:** Lu, Z., Qin, G., Gan, S., Liu, H., Macreadie, P. I., Cheah, W., & Wang, F. (2024). Blue carbon sink capacity of mangroves determined by leaves and their associated microbiome. *Global Change Biology*, *30*, e17007. https://doi.org/10.1111/gcb.17007